

# Nonlocal and cascaded effects in nonlinear graphene nanoplasmonics

– SUPPLEMENTARY INFORMATION –

Theis P. Rasmussen,<sup>1</sup> A. Rodríguez Echarri,<sup>2</sup> F. Javier García de Abajo,<sup>2,3</sup> and Joel D. Cox<sup>1,4,\*</sup>

<sup>1</sup>*Center for Nano Optics, University of Southern Denmark, Campusvej 55, DK-5230 Odense M, Denmark*

<sup>2</sup>*ICFO-Institut de Ciències Fotoniques, The Barcelona Institute of Science and Technology, 08860 Castelldefels (Barcelona), Spain*

<sup>3</sup>*ICREA-Institució Catalana de Recerca i Estudis Avançats, Passeig Lluís Companys 23, 08010 Barcelona, Spain*

<sup>4</sup>*Danish Institute for Advanced Study, University of Southern Denmark, Campusvej 55, DK-5230 Odense M, Denmark*

(Dated: December 15, 2022)

We elaborate on the theoretical formalism presented in the main text with further details pertaining to the specific geometry of nanoribbons that have translational symmetry in one dimension, for which we provide a prescription to obtain self-consistent solutions of the constitutive relations that describe the linear and nonlinear optical response. We additionally summarize the second- and third-order nonlinear conductivities of extended graphene obtained as perturbative solutions to the Boltzmann transport equation. Finally, we present results for second-harmonic generation from stacked graphene nanoribbon dimers that elucidate the roles of plasmon hybridization and lateral positioning.

## CONTENTS

S1. Optical response of nanoribbons	1
A. Linear response	1
B. Real space discretization and matrix formalism	2
C. Nonlinear response	3
S2. Nonlinear optical response of free electrons in graphene	4
S3. Hybridization effects in stacked ribbons	7
References	8

## S1. OPTICAL RESPONSE OF NANORIBBONS

The theoretical formalism presented in the main text to describe the optical response of composite two-dimensional (2D) nanostructures applies to collections of arbitrary morphologies with sizes well below the wavelength of the applied electromagnetic field (i.e., in the quasistatic limit). Here, we consider the specific case of a system of  $N$  ribbons that is translationally invariant in  $\hat{\mathbf{y}}$ , while ribbon  $j \in \{1, 2, \dots, N\}$  of width  $W_j$  occupies a finite region  $x \in \{x_j - W_j/2, x_j + W_j/2\}$  in the plane defined by  $z = z_j$ , such that  $x_j$  is the  $x$ -coordinate of the ribbon center.

### A. Linear response

To linear order, we characterize the optical response of the 2D nanostructure ensemble by the scalar potential  $\Phi(\mathbf{r})$  produced in response to an external potential  $\Phi^{\text{ext}}(\mathbf{r})$ , where a harmonic time dependence  $e^{-i\omega t}$  is assumed. To exploit the symmetry in  $\hat{\mathbf{y}}$ , we decompose the scalar potential in plane waves characterized by wave vector  $q$  according to  $\Phi(\mathbf{r}) = \phi(x, z)e^{iqy}$ , so that Eq. (1) in the main text becomes

$$\phi(x, z)e^{iqy} = \phi^{\text{ext}}(x, z)e^{iqy} + \sum_{j=1}^N \int_{-\infty}^{\infty} dy' \int_{x_j - W_j/2}^{x_j + W_j/2} dx' \frac{\rho_j^{\text{ind}}(x')e^{iqy'}}{\sqrt{(x - x')^2 + (y - y')^2 + (z - z_j)^2}}, \quad (\text{S1})$$

---

\* Joel D. Cox: [cox@mci.sdu.dk](mailto:cox@mci.sdu.dk)

where  $\rho_j^{\text{ind}}$  is the 2D induced charge density in ribbon  $j$ . Invoking the continuity equation  $i\omega\rho_j^{\text{ind}} = \nabla_{\mathbf{R}} \cdot \mathbf{j}_j$  and Ohm's law  $\mathbf{j}_j = \sigma_j^{(1,1)} f_j \mathbf{E}$ , we find

$$\rho_j^{\text{ind}}(x) = \frac{i}{\omega} \sigma_j^{(1,1)}(\omega) \{ \partial_x [f_j(x) \partial_x \phi(x, z_j)] - q^2 f_j(x) \phi(x, z_j) \}, \quad (\text{S2})$$

such that the geometry of the ribbon is defined by  $f_j(x) = 1$  within the region of  $x$  occupied by ribbon  $j$ —where the intrinsic linear conductivity is  $\sigma_j^{(1,1)}$ —and is zero otherwise. Combining Eqs. (S1) and (S2), we perform the integration over  $y'$  to obtain the self-consistent equation

$$\phi(x, z) = \phi^{\text{ext}}(x, z) + 2 \sum_{j=1}^N \frac{i\sigma_j^{(1,1)}}{\omega} \int_{x_j - W_j/2}^{x_j + W_j/2} dx' K_0 \left[ q \sqrt{(x - x')^2 + (z - z_j)^2} \right] \{ \partial_{x'} [f_j(x') \partial_{x'} \phi(x', z_j)] - q^2 f_j(x') \phi(x', z_j) \}.$$

The expression above for the potential in ribbon  $j$  is then recast into the form of Eq. (5) of the main text:

$$\phi_j = \phi_j^{\text{ext}} + \sum_{j'=1}^N \eta_j^{(1)} \mathcal{V}_{jj'}^{(q)} \mathcal{D}_{j'}^{(q)} \phi_{j'}, \quad (\text{S3})$$

where the dimensionless parameter  $\eta_j^{(1)} = i\sigma_j^{(1,1)}/\omega W_j$  contains dependencies on the intrinsic linear conductivity and width, while the integral operator

$$\mathcal{V}_{jj'}^{(q)} g(\theta) = 2 \int_{-1/2}^{1/2} d\theta' K_0 \left[ q \sqrt{(x_{jj'} + W_j \theta - W_{j'} \theta')^2 + z_{jj'}^2} \right] g(\theta') \quad (\text{S4})$$

and the Laplacian operator

$$\mathcal{D}_j^{(q)} g(\theta) = \partial_\theta [f_j(\theta) \partial_\theta g(\theta)] - q^2 W_j^2 f_j(\theta) g(\theta)$$

are expressed in terms of normalized  $x$  coordinates  $\theta \in [-1/2, 1/2]$ , with  $x_{jj'} \equiv x_j - x_{j'}$  and  $z_{jj'} \equiv z_j - z_{j'}$  defining the center-to-center separation of ribbons  $j$  and  $j'$  in the  $\hat{\mathbf{x}}$  and  $\hat{\mathbf{z}}$  directions, respectively. To solve Eq. (S3), we discretize  $\theta$  and the potential  $\phi_j(\theta)$  on a real space grid to construct a vector  $\vec{\phi} = (\phi_1, \phi_2, \dots, \phi_N)^T$  by concatenating the vectors  $\phi_j$ , such that  $\vec{\phi}$  satisfies the matrix equation

$$\vec{\phi} = (\mathbb{1} - \mathcal{M})^{-1} \vec{\phi}^{\text{ext}}, \quad (\text{S5})$$

where  $\mathbb{1}$  denotes the identity matrix,  $\mathcal{M}$  is a square block matrix with elements  $\mathcal{M}_{jj'} = \eta_j^{(1)} \mathcal{V}_{jj'}^{(q)} \mathcal{D}_{j'}^{(q)}$ , and  $\vec{\phi}^{\text{ext}}$  is defined similarly to  $\vec{\phi}$ . In the following subsection, we elaborate on the discretization procedure and matrix representation of the operators  $\mathcal{V}_{jj'}^{(q)}$  and  $\mathcal{D}_j^{(q)}$  for ribbons.

## B. Real space discretization and matrix formalism

To solve Eq. (S3), we discretize  $\theta_j \equiv x/W_j$  for  $x$ -coordinates in ribbon  $j$  into  $L_j$  elements on a one-dimensional spatial grid  $\theta_{j,l} = \{\theta_{j,1}, \theta_{j,2}, \dots, \theta_{j,L_j}\}$ , so that the Coulomb operator becomes a matrix with elements

$$\mathcal{V}_{jj',ll'}^{(q)} = 2 \int_{\theta_{j',l'} - h_{j'}/2}^{\theta_{j',l'} + h_{j'}/2} d\theta' K_0 \left[ q \sqrt{(x_{jj'} + W_j \theta_{j,l} - W_{j'} \theta')^2 + z_{jj'}^2} \right], \quad (\text{S6})$$

where  $h_j = 1/(L_j - 1)$  quantifies the (uniform) spatial discretization, on which scale the function  $g(\theta)$  in Eq. (S4) is assumed to vary slowly, while the matrix representation of the Laplacian operator is

$$\mathcal{D}_{j,ll'}^{(q)} = \frac{1}{2h^2} [\delta_{l-1,l'} (f_{j,l-1} + f_{j,l}) - \delta_{ll'} (f_{j,l-1} + 2f_{j,l} + f_{j,l+1}) + \delta_{l+1,l'} (f_{j,l+1} + f_{j,l})] - \delta_{ll'} q^2 W_j^2 f_{j,l}$$

for elements  $1 < l < L$ , where  $f_{j,l} \equiv f_j(\theta_{j,l})$ , and

$$\begin{aligned} \mathcal{D}_{j,1l'}^{(q)} &= \frac{1}{2h^2} (f_{j,1} + f_{j,2}) (-\delta_{1l'} + \delta_{2l'}) - \delta_{1l'} f_{j,1} q^2 W_j^2, \\ \mathcal{D}_{j,Ll'}^{(q)} &= \frac{1}{2h^2} (f_{j,L-1} + f_{j,L}) (\delta_{L-1,l'} - \delta_{Ll'}) - \delta_{Ll'} f_{j,L} q^2 W_j^2, \end{aligned}$$

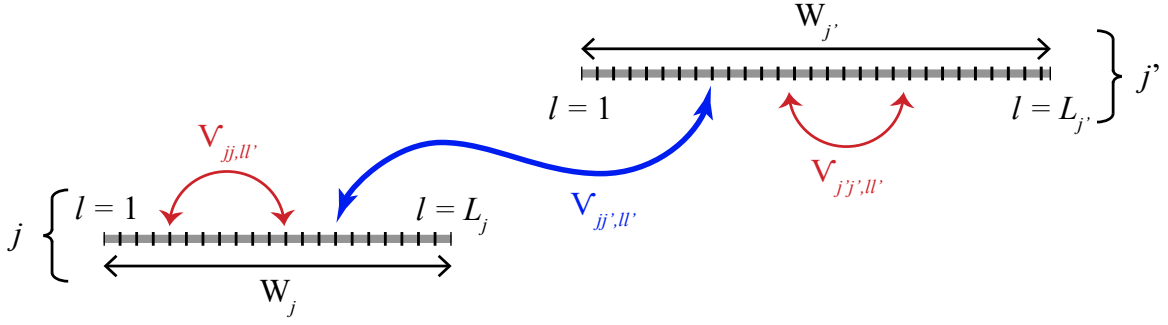


FIG. S1. **Intra- and inter-ribbon coupling between discrete spatial elements.** Ribbon  $j$  of width  $W_j$  is discretized in  $N_j$  real space elements indexed by  $l$  which interact amongst themselves (red arrows) and with their counterparts in another ribbon  $j'$  (blue arrows) through the Coulomb operators  $V_{jj',ll'}$  containing any information pertaining to the inter-ribbon separation.

such that the normal current properly vanishes at the edges of each ribbon [1]. In Fig. S1 we present a schematic illustration of the intra- and inter-ribbon interaction between discretized elements in ribbons  $j$  and  $j'$ . Under specific circumstances, the integral of Eq. (S6) admits analytical solutions. In particular, for finite in-plane wave vector  $q$  and co-planar ribbons, we take  $z_{jj'} = 0$  to obtain

$$V_{jj',ll'}^{(q)} = \pi \sum_{\pm} (\pm) |\theta_{jj',ll'} \pm h/2| \left[ K_0(Q_{j'} |\theta_{jj',ll'} \pm h/2|) \mathcal{L}_{-1}(Q_{j'} |\theta_{jj',ll'} \pm h/2|) \right. \\ \left. + K_1(Q_{j'} |\theta_{jj',ll'} \pm h/2|) \mathcal{L}_0(Q_{j'} |\theta_{jj',ll'} \pm h/2|) \right],$$

where  $Q_{j'} \equiv qW_{j'}$ ,  $\theta_{jj',ll'} \equiv (x_{jj'} + W_j \theta_{j,l} - W_{j'} \theta_{j',l'}) / W_{j'}$ , and  $\mathcal{L}_n$  denotes the modified Struve function of order  $n$  [2], while, for vanishing wave vector  $q = 0$ , Eq. (S6) is evaluated as

$$V_{jj',ll'}^{(0)} = 2 \sum_{\pm} (\pm) \left\{ (\theta_{jj',ll'} \pm h/2) \left[ 1 - \log \sqrt{(\theta_{jj',ll'} \pm h/2)^2 + \tilde{z}_{jj'}^2} \right] - \tilde{z}_{jj'} \tan^{-1} \left( \frac{\theta_{jj',ll'} \pm h/2}{\tilde{z}_{jj'}} \right) \right\},$$

where  $\tilde{z}_{jj'} \equiv z_{jj'} / W_{j'}$ . The solution to Eq. (S3) is then obtained in terms of the elements  $\phi_{j,l} = \phi_j(\theta_l)$  by concatenating the vectors  $\phi_j$  as  $\vec{\phi} = (\phi_1, \phi_2, \dots, \phi_N)^T$  (similarly for  $\vec{\phi}^{\text{ext}}$ ) and defining the square block matrix comprised of matrices  $\mathcal{M}_{jj'} = \eta_{jj'}^{(1)} \mathcal{V}_{jj'}^{(q)} \mathcal{D}_{j'}^{(q)}$  to write Eq. (S5). The potential satisfying Eq. (S3) can then be used to compute the associated linear response from the induced dipole moment, and, as explained in the following section, is used to determine the nonlinear response on the same real space grid.

### C. Nonlinear response

Generally, the quantities that characterize the optical response of the 2D nanostructure ensemble can be decomposed in perturbation orders  $n$  and frequency harmonics  $s$  of the external field according to

$$\Phi(\mathbf{r}, t) = \sum_{n=1}^{\infty} \sum_{s=-n}^n \Phi^{(n,s)}(\mathbf{r}) e^{-is\omega t}$$

for the potential, with components

$$\Phi^{(n,s)}(\mathbf{r}) = \Phi^{\text{ext}}(\mathbf{r}) \delta_{n,1} (\delta_{s,-1} + \delta_{s,1}) + \sum_{j=1}^N \int d^3 \mathbf{r}' \frac{\rho_j^{(n,s)}(\mathbf{R})}{|\mathbf{r} - \mathbf{r}'|} \delta(z' - z_j)$$

that yield the associated electric field  $\mathbf{E}^{(n,s)} = -\nabla \Phi^{(n,s)}$ . Writing the nonlinear current within structure  $j$  as

$$\mathbf{j}_j^{(n,s)} = f_j \sigma_j^{(1,s)} \mathbf{E}^{(n,s)} + \mathbf{j}_{j,\text{NL}}^{(n,s)},$$

where the first term on the left-hand side accounts for the linear response to the nonlinear field  $\mathbf{E}^{(n,s)}$  generated in the structure by the *source* current  $\mathbf{j}_{j,\text{NL}}^{(n,s)}$  associated with a particular nonlinear process, we invoke the continuity equation

$\nabla_{\mathbf{R}} \cdot \mathbf{j}_j^{(n,s)} = i s \omega \rho_j^{(n,s)}$  to obtain the self-consistent integro-differential equation

$$\rho_j^{(n,s)}(\mathbf{R}) = \rho_{j,\text{NL}}^{(n,s)}(\mathbf{R}) + \frac{i}{s\omega} \nabla_{\mathbf{R}} \cdot \left[ f_j(\mathbf{R}) \sigma_j^{(1,s)} \sum_{j'=1}^N \nabla_{\mathbf{R}} \int dy' \int_{x_{j'}-W_{j'}/2}^{x_{j'}+W_{j'}/2} dx' \frac{\rho_{j'}^{(n,s)}(\mathbf{R})}{\sqrt{(x-x')^2 + (y-y')^2 + (z_j - z_{j'})^2}} \right], \quad (\text{S8})$$

where  $\rho_{j,\text{NL}}^{(n,s)} = -(i/s\omega) \nabla_{\mathbf{R}} \cdot \mathbf{j}_{j,\text{NL}}^{(n,s)}$ . For an ensemble of nanoribbons with translational invariance in  $\hat{\mathbf{y}}$ , we follow the procedure described above for the linear optical response to express Eq. (S8) in the form

$$\rho_j^{(n,s)} = \rho_{j,\text{NL}}^{(n,s)} + \eta_j^{(s)} \mathcal{D}_j^{(sq)} \sum_{j'} \frac{W_{j'}}{W_j} \mathcal{V}_{jj'}^{(sq)} \rho_{j'}^{(n,s)}, \quad (\text{S9})$$

where  $\eta_j^{(s)} = i\sigma^{(1,s)}/s\omega W_j$  is a dimensionless parameter. The solution to Eq. (S9) is then obtained by adopting the discretization procedure discussed in the previous sections and expressing the combined charge density  $\vec{\rho}^{(n,s)} = (\rho_1^{(n,s)}, \rho_2^{(n,s)}, \dots, \rho_N^{(n,s)})^T$  in a matrix equation as

$$\vec{\rho}^{(n,s)} = (\mathbb{1} - \mathcal{N})^{-1} \vec{\rho}_{\text{NL}}^{(n,s)},$$

where the block matrix  $\mathcal{N}$  is comprised of matrices  $\mathcal{N}_{jj'} = \eta_j^{(s)} W_{j'} W_j^{-1} \mathcal{D}_j^{(sq)} \mathcal{V}_{jj'}^{(sq)}$ .

## S2. NONLINEAR OPTICAL RESPONSE OF FREE ELECTRONS IN GRAPHENE

The optical response of highly-doped graphene is well described within the theoretical framework of the Boltzmann transport equation in the relaxation-time approximation [3], which yields compact analytical expressions for the intrinsic nonlinear optical conductivity associated with intraband charge carrier motion in the carbon monolayer. In what follows we adopt the procedure of Ref. [4] to derive the nonlinear optical conductivity in both the second- and third-order response to monochromatic illumination  $\mathbf{E}(\mathbf{R}, t) = \mathbf{E}(\mathbf{R}) e^{-i\omega t} + \text{c.c.}$ , where  $\mathbf{R} = (x, y)$  denotes the plane occupied by an infinitely-extended graphene sheet. The equation of motion for the 2D electron distribution  $f_{\mathbf{k}}(\mathbf{R}, t)$  is

$$\frac{df_{\mathbf{k}}}{dt} = \frac{\partial f_{\mathbf{k}}}{\partial t} + \nabla_{\mathbf{p}} f_{\mathbf{k}} \cdot \frac{d\mathbf{p}}{dt} + \nabla_{\mathbf{R}} f_{\mathbf{k}} \cdot \frac{d\mathbf{R}}{dt} = -\gamma (f_{\mathbf{k}} - f_{\mathbf{k}}^{(0)}), \quad (\text{S10})$$

where the electron momentum  $\mathbf{p} = \hbar \mathbf{k}$  is related to the in-plane wave vector  $\mathbf{k}$ , and we include a phenomenological damping term that relaxes the system to an equilibrium state  $f_{\mathbf{k}}^{(0)}$  at a rate  $\gamma = \tau^{-1}$ . Inserting the Lorentz force in Newton's second law, we write the rate of change of the momentum as

$$\frac{d\mathbf{p}}{dt} = -e \left[ \mathbf{E}(\mathbf{R}, t) + \frac{1}{c} \frac{d\mathbf{R}}{dt} \times \mathbf{B}(\mathbf{R}, t) \right],$$

while the electron velocity is governed by the linearized dispersion relation of electrons in the vicinity of the Dirac points in graphene  $d\mathbf{R}/dt = \pm v_F \mathbf{k}/k$ , where the positive (negative) sign corresponds to electron (hole) doping. Combining the above expressions, Eq. (S10) becomes

$$\frac{\partial f_{\mathbf{k}}}{\partial t} = \frac{e}{\hbar} \left[ \mathbf{E}(\mathbf{R}, t) \pm \frac{v_F}{c} \frac{\mathbf{k}}{k} \times \mathbf{B}(\mathbf{R}, t) \right] \cdot \nabla_{\mathbf{k}} f_{\mathbf{k}} \mp v_F \frac{\mathbf{k}}{k} \cdot \nabla_{\mathbf{R}} f_{\mathbf{k}} - \gamma (f_{\mathbf{k}} - f_{\mathbf{k}}^{(0)}), \quad (\text{S11})$$

the solution of which is expanded in powers of the external field according to

$$f_{\mathbf{k}}(\mathbf{R}, t) = \sum_{n=0}^{\infty} \sum_{s=-n}^n f_{\mathbf{k}}^{(n,s)}(\mathbf{R}) e^{-is\omega t}, \quad \mathbf{E}(\mathbf{R}, t) = \sum_{n=1}^{\infty} \sum_{s=-n}^n \mathbf{E}^{(n,s)}(\mathbf{R}) e^{-is\omega t}, \quad (\text{S12})$$

such that the perturbation order  $n$  and harmonic index  $s$  necessarily satisfy  $|s| \leq n$ , while  $f_{\mathbf{k}}^{(n,-s)} = (f_{\mathbf{k}}^{(n,s)})^*$  and  $\mathbf{E}^{(n,-s)} = (\mathbf{E}^{(n,s)})^*$ . Inserting Eq. (S12) into Eq. (S11) and equating terms of order  $n > 0$  and harmonic  $s$ , we find

$$f_{\mathbf{k}}^{(n,s)} = \frac{ie}{\hbar} \left( s\omega + i\gamma \pm i v_F \frac{\mathbf{k}}{k} \cdot \nabla_{\mathbf{R}} \right)^{-1} \sum_{n'=1}^n \sum_{s'=-n'}^{n'} \tilde{\mathbf{E}}^{(n',s')} \cdot \nabla_{\mathbf{k}} f_{\mathbf{k}}^{(n-n',s-s')},$$

where

$$\tilde{\mathbf{E}}^{(n,s)} = \mathbf{E}^{(n,s)} \mp \frac{iv_F}{s\omega} \left[ \nabla_{\mathbf{R}} \left( \frac{\mathbf{k}}{k} \cdot \mathbf{E}^{(n,s)} \right) - \left( \frac{\mathbf{k}}{k} \cdot \nabla_{\mathbf{R}} \right) \mathbf{E}^{(n,s)} \right] \quad (\text{S13})$$

is obtained by eliminating the magnetic field  $\mathbf{B}^{(n,s)} = (ic/s\omega)\nabla_{\mathbf{r}} \times \mathbf{E}^{(n,s)}$  in favor of the electric field.

Crucially, nonlocal effects are incorporated in the optical response by expanding

$$\left( s\omega + i\gamma \pm iv_F \frac{\mathbf{k}}{k} \cdot \nabla_{\mathbf{R}} \right)^{-1} \approx \frac{1}{s\omega + i\gamma} \left[ 1 \mp \frac{iv_F}{s\omega + i\gamma} \frac{\mathbf{k}}{k} \cdot \nabla_{\mathbf{R}} + \dots \right]$$

and retaining only up to the leading term in  $\nabla_{\mathbf{R}}$  to write

$$f_{\mathbf{k}}^{(n,s)} = \frac{ie}{\hbar} D_{s\omega} \left( 1 \mp iv_F D_{s\omega} \frac{\mathbf{k}}{k} \cdot \nabla_{\mathbf{R}} \right) \sum_{n'=1}^n \sum_{s'=-n'}^{n'} \tilde{\mathbf{E}}^{(n',s')} \cdot \nabla_{\mathbf{k}} f_{\mathbf{k}}^{(n-n',s-s')}, \quad (\text{S14})$$

where  $D_{s\omega} = (s\omega + i\gamma)^{-1}$ .

The contribution to the in-plane current  $\mathbf{j}(\mathbf{R}, t) = \sum_{n=1}^{\infty} \sum_{s=-n}^n \mathbf{j}^{(n,s)}(\mathbf{R}) e^{-is\omega t}$  of order  $n$  and harmonic  $s$  in the external field is found by integrating over all electron momenta according to

$$\mathbf{j}^{(n,s)} = \mp ev_F \int \frac{d^2\mathbf{k}}{(2\pi)^2} \frac{\mathbf{k}}{k} f_{\mathbf{k}}^{(n,s)}. \quad (\text{S15})$$

Combining Eqs. (S14) and (S15), we isolate the self-consistent  $n = n'$  term to write the current as

$$\mathbf{j}^{(n,s)} = \mp \frac{ie^2 v_F}{4\pi^2 \hbar} D_{s\omega} \int d^2\mathbf{k} \frac{\mathbf{k}}{k} \left( 1 \mp iv_F D_{s\omega} \frac{\mathbf{k}}{k} \cdot \nabla_{\mathbf{R}} \right) \tilde{\mathbf{E}}^{(n,s)} \cdot \nabla_{\mathbf{k}} f_{\mathbf{k}}^{(0)} + \mathbf{j}_{\text{NL}}^{(n,s)}, \quad (\text{S16})$$

where

$$\mathbf{j}_{\text{NL}}^{(n,s)} = \mp \frac{ie^2 v_F}{4\pi^2 \hbar} D_{s\omega} \sum_{n'=1}^{n-1} \sum_{s'=-n'}^{n'} \int d^2\mathbf{k} \frac{\mathbf{k}}{k} \left( 1 \mp iv_F D_{s\omega} \frac{\mathbf{k}}{k} \cdot \nabla_{\mathbf{R}} \right) \tilde{\mathbf{E}}^{(n',s')} \cdot \nabla_{\mathbf{k}} f_{\mathbf{k}}^{(n-n',s-s')} \quad (\text{S17})$$

is the intrinsic nonlinear response constructed from lower perturbation orders  $n' < n$ . From the unperturbed electronic distribution of graphene at zero temperature  $f_{\mathbf{k}}^{(0)} = 4\Theta(\pm k_F \mp k)$ , where  $k_F = E_F/\hbar v_F$  is the Fermi wave vector and the factor of 4 accounts for spin and valley degeneracies, we evaluate  $\nabla_{\mathbf{k}} f_{\mathbf{k}}^{(0)} = \mp 4(\mathbf{k}/k)\delta(k_F - k)$  and insert Eq. (S13) to write Eq. (S16) as

$$j_i^{(n,s)} = \sigma_{ij}^{(1,s)} E_j^{(n,s)} + j_{\text{NL},i}^{(n,s)}, \quad (\text{S18})$$

here expressed using the Einstein summation convention for vector components spanning the  $x$  and  $y$  directions such that  $\{i, j\} \in \{x, y\}$ . The first term arises from the  $n' = n$  contribution in the summation of Eq. (S14) and describes the linear response to the induced nonlinear field at harmonic  $s$  mediated by the conductivity

$$\sigma_{ij}^{(1,s)} = \frac{ie^2}{\pi \hbar^2} \frac{E_F}{s\omega + i\gamma} \delta_{ij},$$

whereas the second term (contributing when  $n > 1$ ) is

$$j_{\text{NL},i}^{(n,s)} = \mp \frac{ie^2 v_F}{4\pi^2 \hbar} D_{s\omega} \sum_{n'=1}^{n-1} \sum_{s'=-n'}^{n'} \int d^2\mathbf{k} \left[ \begin{aligned} & \left( \frac{\delta_{ij}}{k} - \frac{k_i k_j}{k^3} \right) E_j^{(n',s')} f_{\mathbf{k}}^{(n-n',s-s')} \\ & \mp iv_F D_{s\omega} \left( \frac{\delta_{il} k_j}{k^2} + \frac{\delta_{jl} k_i}{k^2} - 2 \frac{k_i k_j k_l}{k^4} \right) \partial_{\mathbf{R},j} \left( E_l^{(n',s')} f_{\mathbf{k}}^{(n-n',s-s')} \right) \\ & \mp \frac{iv_F}{s'\omega} \left( \frac{\delta_{il} k_j}{k^2} + \frac{\delta_{jl} k_i}{k^2} - 2 \frac{k_i k_j k_l}{k^4} \right) \left( \partial_{\mathbf{R},l} E_j^{(n',s')} - \partial_{\mathbf{R},j} E_l^{(n',s')} \right) f_{\mathbf{k}}^{(n-n',s-s')} \end{aligned} \right]. \quad (\text{S19})$$

In obtaining the current of Eq. (S18), terms beyond linear order in  $\nabla_{\mathbf{R}}$  are omitted, while the  $k$ -space integration is performed according to the procedure of Ref. 4 (i.e., integrating by parts in Eq. (S17) to avoid derivatives of  $\delta(k_F - k)$ ), with odd-rank tensors vanishing in the azimuthal integration.

For the current associated with second-harmonic generation (SHG), we choose  $n = s = 2$  in Eq. (S19) to recover the result of Eq. (11) in the main text:

$$\mathbf{j}_{\text{NL}}^{(2,2)} = \sigma_{\text{A}}^{(2,2)} \mathbf{E}^{(1,1)} \left( \nabla_{\mathbf{R}} \cdot \mathbf{E}^{(1,1)} \right) + \sigma_{\text{B}}^{(2,2)} \left( \mathbf{E}^{(1,1)} \cdot \nabla_{\mathbf{R}} \right) \mathbf{E}^{(1,1)} + \sigma_{\text{C}}^{(2,2)} \nabla_{\mathbf{R}} \left( \mathbf{E}^{(1,1)} \cdot \mathbf{E}^{(1,1)} \right), \quad (\text{S20})$$

where

$$\begin{aligned} \sigma_{\text{A}}^{(2,2)} &= \mp S^{(2)} D_{2\omega} D_{\omega} (3D_{\omega} + 4D_{2\omega}) \\ \sigma_{\text{B}}^{(2,2)} &= \mp S^{(2)} D_{2\omega} D_{\omega} \left( -D_{\omega} + 4D_{2\omega} - \frac{4}{\omega} \right) \\ \sigma_{\text{C}}^{(2,2)} &= \mp S^{(2)} D_{2\omega} D_{\omega} \left( -\frac{D_{\omega}}{2} - 2D_{2\omega} + \frac{2}{\omega} \right), \end{aligned}$$

with the prefactor  $S^{(2)} \equiv ie^3 v_{\text{F}}^2 / 4\pi \hbar^2$ .

Up to this point, the derivation of optical response functions describing free electrons in graphene subject to monochromatic illumination parallels that presented in Ref. [4], where the third-order conductivity is also reported in the local limit, i.e., retaining only the first term in Eq. (S18) for  $n = s = 3$ . Here we supplement the result for third-harmonic generation (THG) obtained in Ref. [4] by including nonlocal terms in Eq. (S18). After performing straightforward but lengthy mathematical manipulations, we obtain the result presented in Eq. (13) of the main text,

$$\mathbf{j}_{\text{NL}}^{(3,3)} = \sigma^{(3,3)} \mathbf{E}^{(1,1)} \left( \mathbf{E}^{(1,1)} \cdot \mathbf{E}^{(1,1)} \right) + \mathbf{j}_{\text{NL}}^{(2,\{1,2\})}, \quad (\text{S22})$$

where  $\sigma^{(3,3)} = (3ie^4 v_{\text{F}}^2 / 4\pi \hbar^2 E_{\text{F}}) D_{3\omega} D_{2\omega} D_{\omega}$  is the local third-order THG conductivity and

$$\begin{aligned} \mathbf{j}_{\text{NL}}^{(2,\{1,2\})} &= \sigma_{\text{A}}^{(2,1,2)} \mathbf{E}^{(1,1)} \left( \nabla_{\mathbf{R}} \cdot \mathbf{E}^{(2,2)} \right) + \sigma_{\text{A}}^{(2,2,1)} \mathbf{E}^{(2,2)} \left( \nabla_{\mathbf{R}} \cdot \mathbf{E}^{(1,1)} \right) \\ &+ \sigma_{\text{B}}^{(2,1,2)} \left( \mathbf{E}^{(1,1)} \cdot \nabla_{\mathbf{R}} \right) \mathbf{E}^{(2,2)} + \sigma_{\text{B}}^{(2,2,1)} \left( \mathbf{E}^{(2,2)} \cdot \nabla_{\mathbf{R}} \right) \mathbf{E}^{(1,1)} \\ &+ \sigma_{\text{C}}^{(2,1,2)} \sum_{j=x,y} E_j^{(1,1)} \nabla_{\mathbf{R}} E_j^{(2,2)} + \sigma_{\text{C}}^{(2,2,1)} \sum_{j=x,y} E_j^{(2,2)} \nabla_{\mathbf{R}} E_j^{(1,1)} \\ &+ \sigma_{\text{D}}^{(2,1,2)} \nabla_{\mathbf{R}} \left( \mathbf{E}^{(1,1)} \cdot \mathbf{E}^{(2,2)} \right), \end{aligned}$$

with

$$\begin{aligned} \sigma_{\text{A}}^{(2,s_1,s_2)} &= \mp S^{(2)} D_{(s_1+s_2)\omega} \left[ 3D_{s_2\omega}^2 + 2D_{(s_1+s_2)\omega} (D_{s_1\omega} + D_{s_2\omega}) \right], \\ \sigma_{\text{B}}^{(2,s_1,s_2)} &= \mp S^{(2)} D_{(s_1+s_2)\omega} \left[ 2D_{(s_1+s_2)\omega} (D_{s_1\omega} + D_{s_2\omega}) - D_{s_2\omega}^2 - \frac{4D_{s_1\omega}}{s_2\omega} \right], \\ \sigma_{\text{C}}^{(2,s_1,s_2)} &= \mp S^{(2)} D_{(s_1+s_2)\omega} \left( \frac{4D_{s_1\omega}}{s_2\omega} - D_{s_2\omega}^2 \right), \\ \sigma_{\text{D}}^{(2,s_1,s_2)} &= \pm 2S^{(2)} D_{(s_1+s_2)\omega}^2 (D_{s_1\omega} + D_{s_2\omega}). \end{aligned}$$

The second term in Eq. (S22) accounts for the second-order mixing of the second-harmonic and fundamental near fields, and corresponds to the so-called *cascaded* contribution to THG.

Note that for impinging light polarized entirely along  $\hat{\mathbf{x}}$  and without any oblique optical momentum component in  $\hat{\mathbf{y}}$ , such that  $q = 0$ , the nonlinear current of Eqs. (S20) and (S22) reduce to

$$j_{\text{NL},x}^{(2,2)} = \mp S^{(2)} D_{2\omega} D_{\omega} (D_{\omega} + 4D_{2\omega}) E_x^{(1,1)} \partial_x E_x^{(1,1)}$$

and

$$j_{\text{NL},x}^{(3,3)} = \sigma^{(3,3)} \left[ E_x^{(1,1)} \right]^3 \mp S^{(2)} D_{3\omega} \left\{ [D_{2\omega}^2 + 2D_{3\omega} (D_{2\omega} + D_{\omega})] E_x^{(1,1)} \partial_x E_x^{(2,2)} + [D_{\omega}^2 + 2D_{3\omega} (D_{2\omega} + D_{\omega})] E_x^{(2,2)} \partial_x E_x^{(1,1)} \right\}.$$

### S3. HYBRIDIZATION EFFECTS IN STACKED RIBBONS

If the illumination frequency is fixed to the dipole plasmon resonance of ribbon  $j = 1$ , a second ribbon can enhance harmonic generation at order  $s$  in a ribbon dimer when the condition  $E_{F2}/E_{F1} = s^2 W_2 \eta_m / W_1 \eta_1$  is satisfied, where  $\eta_m$  denotes the eigenvalue associated with the  $m^{\text{th}}$ -order ribbon eigenmode. However, when ribbons are in close proximity, hybridization effects leads to shifts in the resonance frequencies that change the optimal conditions for harmonic generation in the  $(W_j, E_{Fj})$  parameter space. In Fig. S2 we present the SHG susceptibility of the stacked ribbon dimer considered in Fig. 2 of the main text, for which the  $j = 1$  ribbon has width  $W_1 = 160$  nm and doping  $E_{F1}$ , while the parameters of ribbon  $j = 2$  are varied. In particular, panels (a-d) are obtained for separations  $d = 2.5$  nm,  $d = 5$  nm,  $d = 25$  nm, and  $d = 100$  nm, respectively, while the dashed, dot-dashed, and solid lines indicate the  $\omega_{p1} = \omega_{p2}/2$  resonance conditions for the  $m = 1$ ,  $m = 2$ , and  $m = 3$  modes, respectively.

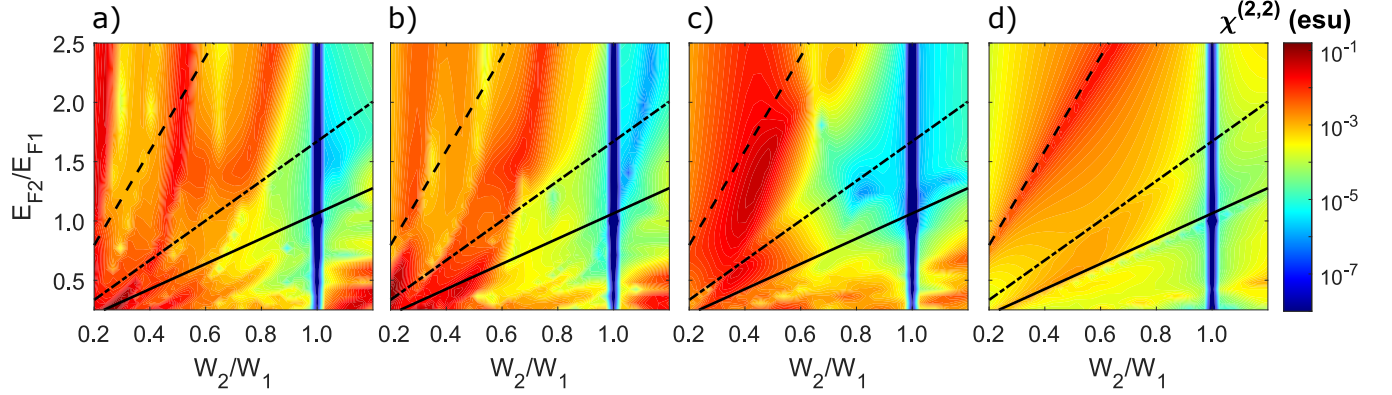


FIG. S2. **Plasmon hybridization in second-harmonic generation from stacked ribbon dimers.** SHG susceptibility of a stacked ribbon pair separated by (a)  $d = 2.5$  nm, (b)  $d = 5$  nm, (c)  $d = 25$  nm, and (d)  $d = 100$  nm when the illumination frequency is fixed to the lowest-order dipolar plasmon resonance of ribbon  $j = 1$  with  $W_1 = 160$  nm and  $E_{F1} = 0.4$  eV while the width and doping of ribbon  $j = 2$  are varied. The dashed, dot-dashed, and solid curves indicate the SHG resonance condition for the eigenmodes  $\eta_1$ ,  $\eta_2$ , and  $\eta_3$ , respectively. The ribbons are self-standing in vacuum.

Next, we seek to identify the optimal horizontal positioning of two stacked graphene ribbons by changing center-to-center distance  $\Delta x$  in the  $\hat{x}$ -direction, such that the SHG response vanishes due to symmetry when  $\Delta x = 0$ . In Fig. S3(a-d), we consider the effect of horizontal positioning for two ribbons of common doping  $E_{F1} = E_{F2} = 0.4$  eV and different widths  $W_1 = 160$  nm and  $W_2 = 40$  nm for vertical separations (b)  $d = 5$  nm, (c)  $d = 25$  nm, and (d)  $d = 100$  nm, while in Fig. S3(e-f) we choose two ribbons of common width  $W_1 = W_2 = 100$  nm and different doping levels  $E_{F1} = 0.2$  eV and  $E_{F2} = 0.8$  eV for separations (e)  $d = 2.5$  nm, (f)  $d = 5$  nm, and (g)  $d = 25$  nm.

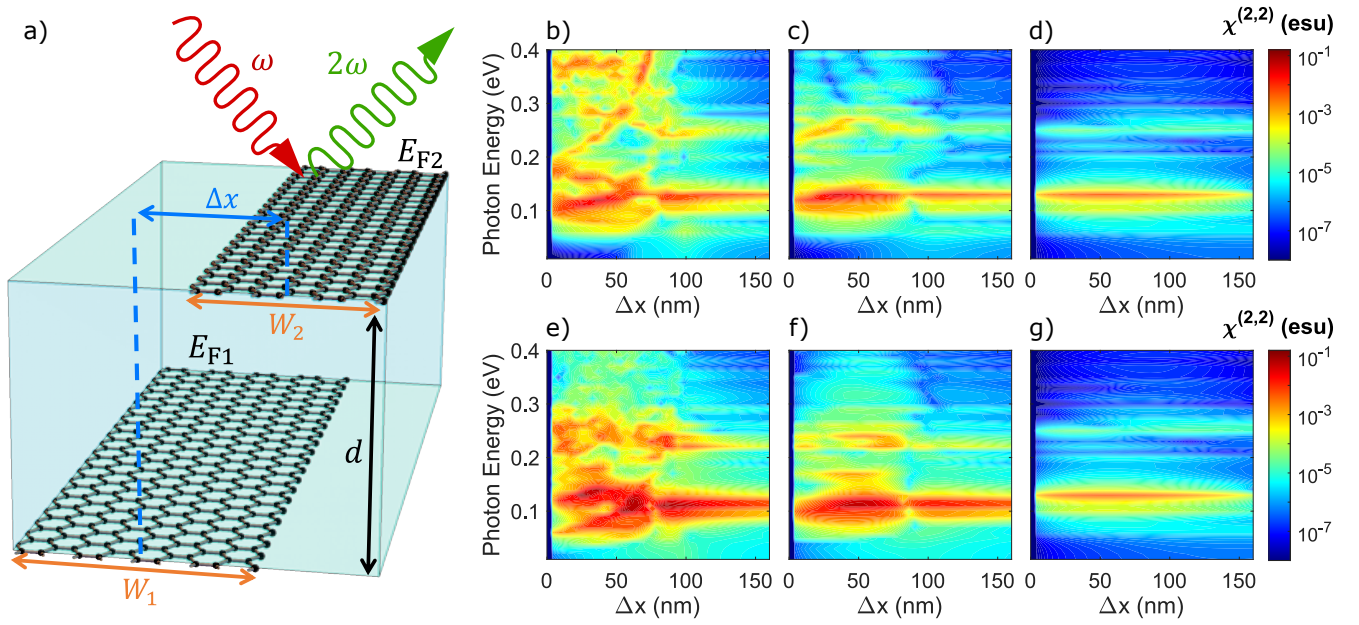


FIG. S3. **Horizontal positioning in second-harmonic generation from stacked ribbon dimers.** (a) Schematic illustration of two parallel graphene ribbons with widths  $W_1$  and  $W_2$  doped to  $E_{F1}$  and  $E_{F2}$  that are separated by a vertical distance  $d$  and offset horizontally by the center-to-center distance  $\Delta x$ . (b-d) SHG response of two ribbons with widths  $W_1 = 160$  nm and  $W_2 = 40$  nm and doping levels  $E_{F1} = E_{F2} = 0.4$  eV as a function of excitation energy and horizontally shifted distance  $\Delta x$  for (b)  $d = 5$  nm, (c)  $d = 25$  nm, and (d)  $d = 100$  nm. (e-g) Similar to panels (b-d), but for two ribbons of widths  $W_1 = W_2 = 100$  nm and doping levels  $E_{F1} = 0.2$  eV and  $E_{F2} = 0.8$  eV. All results have been computed for damping  $\hbar\gamma = 0.01$  eV and permittivity  $\epsilon = 1$ .

- 
- [1] T. Christensen, W. Yan, A.-P. Jauho, M. Wubs, and N. A. Mortensen, *Phys. Rev. B* **92**, 121407 (2015).  
[2] M. Abramowitz and I. A. Stegun, *Handbook of mathematical functions with formulas, graphs, and mathematical tables*, Vol. 55 (US Government Printing Office, Washington, DC, 1948).  
[3] G. Grosso and G. P. Parravicini, *Solid state physics* (Academic press, 2013).  
[4] J. D. Cox, R. Yu, and F. J. García de Abajo, *Phys. Rev. B* **96**, 045442 (2017).